EFFECT OF WELD PARAMETERS ON MECHANICAL PROPERTIES OF THE FRICTION STIR WELDING AA6063-T5

Tran Hung Tra

Materials science Department, Nha Trang University, Nha Trang, Khanh Hoa, Vietnam, Tel: +84 935272168, e-mail: tra@ntu.edu.vn

Received Date: October 14, 2011

Abstract

Effect of tool rotation speed and welding speed on the mechanical properties of the FSW joint of AA6063-T5 was investigated. The influences of the ratio of rotation speed and weld speed on the weld thermal cycle, hardness distribution, and tensile strength of the FSW joint were clarified. The experimental results showed the lower the ratio of rotation speed and weld speed, the lower weld heat input, the narrower the softened zone and the higher tensile strength were. In all cases, the tensile fracture located outside the stirred zone, in the retreating side or advancing side, where the hardness was lowest. It was also found that the residual stress in and around the welded zone was quite low, in range of ten percent of base metal yield stress.

Keywords*:* Friction stir welding, Hardness, Residual stress, Tensile properties, Thermal cycle

Introduction

Friction stir welding (FSW) is emerging as an appropriate alternative technology with high efficiency due to high-processing speeds. Since the joint can be obtained below the melting temperature, this method is suitable for joining a number of materials which are extremely difficult to be welded by conventional fusion techniques [1-3]. Besides welding, friction stir processing has been developing as a potential metalworking technique for metallic components such as localized microstructure modification, control of microstructures in the near-surface layers [4-7]. The basic concept of FSW is remarkably simple. The rotating shoulder and probe of a non-consumable tool heat and plasticize the surrounding metal and a solid-state joining is accomplished there. There, the tool serves three primary functions (1) heating of the workpiece, (2) movement of material to produce the joint, and (3) containment of the hot metal beneath the tool shoulder [8]. The heating is generated by friction between the rotation tool (shoulder and probe) and the workpiece and by plastic deformation of the workpiece. The localized heating softens material around the tool probe and then combines with the tool shoulder and probe rotation and translation leads to movement of material from the front to the back of the probe to fill the hole in the tool wake as the tool moves forward [8]. The tool shoulder restricts metal flow upward. During FSW process, the welding parameters combined with tool geometry exert a significant effect on the material flow pattern and temperature distribution, thereby influencing the microstructural evolution of material, the formation, and mechanical properties of the joint [1-11]. To broaden the application of FSW, it is necessary to clarify the effect of weld parameters on the properties of the joint. The aim of this work is to investigate the effect of tool rotation speed and weld speed on the mechanical properties of the FSW butt-joint of AA6063-T5 plate.

Experimental Procedures

The 5 mm AA6063-T5 plates were butt-joined by friction stir welding using the 1.5 kW NC milling machine. The weld tool geometry applied in this work is a scrolled shoulder tool and a truncated cone pin with the pin diameter of 5.0 mm at the midle pin length, the pin heigth of 4.5 mm, and the screw pitch of 1.0 mm. The pin is aligned at a tilt angle of 2.0 deg. in the plane containing pin axis and center weld line (the tilt angle is defined as the angle between pin axis and the direction perpendicular to the workpieces). The tool tip is kept at a distance of 0.2 mm from the backing anvil. Various regimes of weld parameters were performed by combining the tool rotation speed (denoted ω, revolving/min) and the weld speed (denoted v, mm/min). The ratio of rotation speed and weld speed (denoted ω/v, revolving/mm) investigated is in range from 3.1 to 37.5 revolving/mm. During the welding, the thermal hysteresis at the end weld center and at the shoulder limit areas in advancing side and retreating side (1.0 mm far from the shoulder limit line) was monitored by the thermal couples attached on the weld surface with a computer software interface. After being fabricated, the microstructure was observed by Scanning Electron Microscope (SEM). The hardness in and around the welded zone was measured by a diamond indentation with 50g loading and 10 sec hold time. The tensile strength of the FSW 6063-T5 was measured by the 3.0 mm thickness plate specimens those were extracted in the perpendicular to the weld direction from the 5.0 mm FSW plate as shown in Fig. 1. In these tensile specimens, the weld surface and root surface were removed with the layers of 1.0 mm thickness. The tensile tests were performed by the MTS hydraulic machine at a constant strain rate of 10^{-3}/s. The residual stress in and around the welded zone of the FSW joint was measured by X-ray diffraction (XRD) method [12] in which the specimen surface of specimens was carefully polished by the electrolytic polisher. In X-ray stress measurement, the stress in the surface layer is in general calculated from the change in the lattice spacing. To determine residual stress through XRD, the X-ray stress constants K of BM was determined through six applied load values corresponding to 0, 15, 30, 45, 60, and 75 percent of yield stress in this work. Assuming that the strain in the crystal lattice is linearly distorted, residual stresses are then calculated by means of the stress constants of the metal. Here, an X-ray tube with a chrome anode operated at 30 kV and 30 mA was used to measure the residual stresses. Measurements were collected at a Bragg angle of 139.5 deg. corresponding to diffraction at the {311} planes. The scanning angle of $2\psi\theta$ is from 137 degrees to 142.5 degrees with step 0.05 degree and preset time (time per measurements) of 10 seconds. At each measured location, the residual stresses was measured in a diffracted area of 2×2 mm^2 on specimen surface. Two residual stress components were measured; one perpendicular to weld direction (denoted by transverse) and the other parallel to weld direction (denoted by longitudinal residual stress).

Experimental Results and Discussion

Several combined regimes of rotation speed and welding speed were performed for fabricating the joints to study the effect of rotation speed and weld speed on the mechanical properties of the FSW joint of aluminum 6063-T5. The typical microstructure of a FSW 6063-T5 (fabricated at ω/v = 3.1 revolving/mm) characterized by the dynamic recystallization was seen in Figure 2. In general, the grain sizes in the stirred zone and base metal were about 15μm and 70μm in diameter, respectively (compare Figure 2(c) with Figure 2(d)). In the stirred zone near the interface area (Figure 2(b)), the microstructure displays an inhomogeneous feature. In the stirred zone, the grain size in region near interface area (region II in Figure 2) seems to be finer than that in the middle of stirred zone (region III in Figure 2); this might associates with the fact that the weld temperature in region II is higher

than that in region III [13]. Outside the stirred zone, the grain is comparable to that of base metal (BM), see Figure 2(a). The fine grain size in the stirred zone is mostly independent to both rotation speed and weld speed. In almost all of the fabricated joints, the formation of zigzag-line pattern (usually called "lazy S") in the stirred zone was found to be inevitable excepting for the FSW fabricated at high value of ω/v, *i.e.* ω/v = 37.5 revolving/mm. It should be noted that, in the case of free zigzag-line pattern FSW, the weld temperature is highest and the weld surface is severely turbulent deformation.

The temperature distribution within and around the stirred zone directly influences the microstructure of the welds, such as grain size, grain boundary character, coarsening and dissolution of precipitates, and resultant mechanical properties of the welds [9-11,14]. It is important to obtain the temperature distribution in and around the welded zone during FSW. However, be noted that direct temperature measurements within the stirred zone are difficult due to the intense plastic deformation produced by the rotation and translation of the pin tool. The results of weld temperature measured at the advancing side, the retreating side and at the weld end center are summarized in Figure 3-5. The dependence of the peak weld temperatures on weld parameters are shown in Figure 3 and 4. Both the rotation speed and the weld speed influence the peak weld temperature there the weld temperature is increased with the increase of rotation speed and/or with the decrease of weld speed, see Figure 3. In all cases, the maximum weld temperature was found at the weld center and the weld temperatures in advancing side and in retreating side seem to be comparable, see Figure 4. Furthermore, the results in Figure 4 showed the peak weld temperatures are proportional correlation to the ratio ω/v. Furthermore, Figure 4 also indicates the weld temperature is proportional to the weld input energy. From this view, it is reasonable to choose the ratio of tool rotation and the weld speed, ω/v, as a weld parameter covering both tool rotation speed and weld speed, and their interaction. Another important aspect seen from Figure 4 is the peak weld temperatures are higher than that of dissolution point and remarkable lower than melting point of this alloy, the dash-lines in Figure 4 (the dissolution point of AA6063-T5 was referred in the literature [14]). The influence of weld parameters on the thermal cycles is shown in Figure 5. It is obviously that weld speed influences significantly the heating rate whereas the rotation speed has a minor effect.

The hardness distributions measured at the middle-line in the cross sections are shown in Figure 6 as a function of weld parameter, ω/v. In general, a softened feature in and around the welded zone is observed in all FSWs. Here, the higher ω/v the higher weld temperature (see Figure 4) and the wider softened zone (see Figure 6) in the FSW were seen. The width of soft zone increases with the increase of ω/v. The softening appearing in and around the welded zone could be relating to the dissolution and/or coarsening of precipitates in this alloy [14]. It was also found that, in all cases, the lowest hardness in the cross section of the FSW is placed at the heat affected zone (HAZ) in the advancing side and/or retreating side, outside the stirred zone (see Figure 7). The fact that the hardness in the stirred zone is higher than that in HAZ might be associated with high density of grain boundaries in the stirred zone or Hall Petch effect [15].

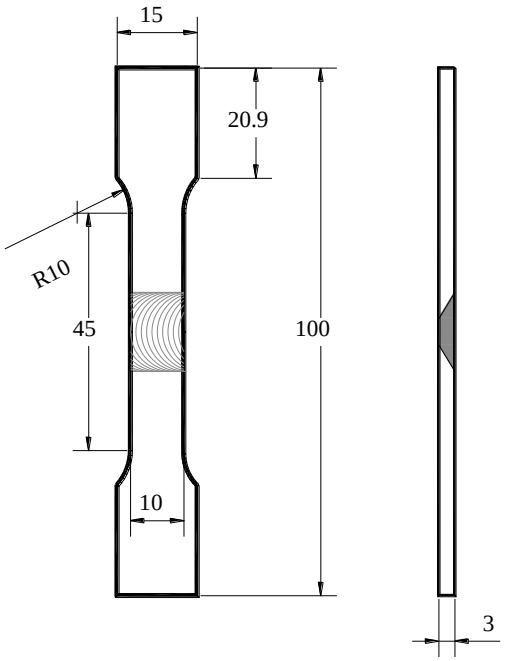

Figure 1. Geometry of tensile specimen

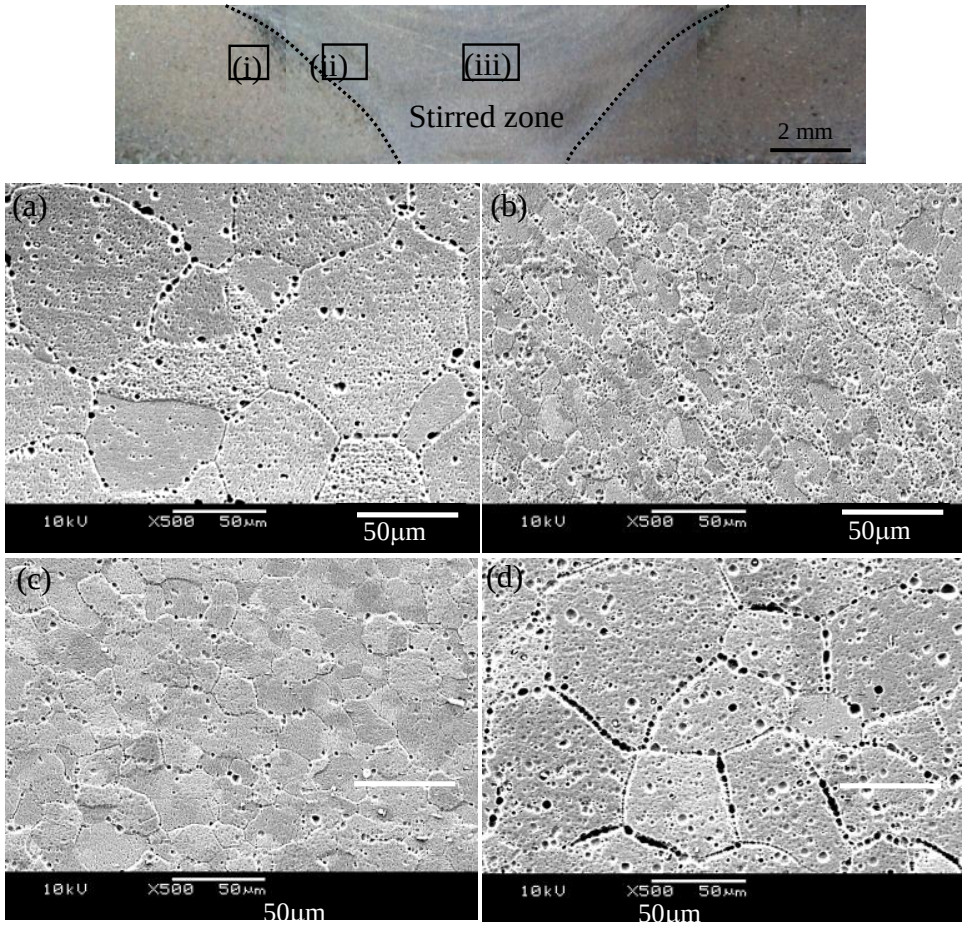

Figure 2. Microstructure in the cross section of FSW No.5; (a) region (i), (b) region (ii), (c) region (iii), and (d) base metal

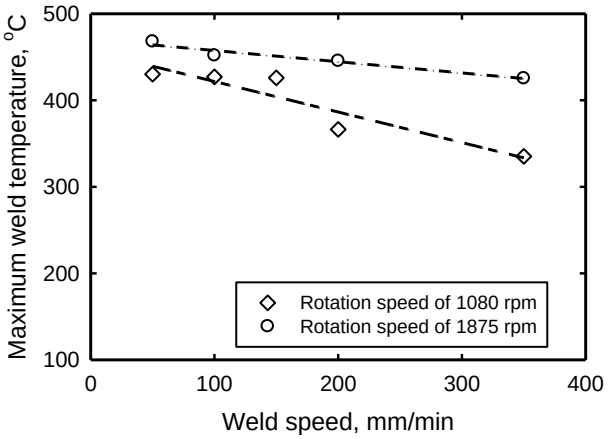

Figure 3. Effect of rotation speed and weld speed on the maximum temperature in the FSWs

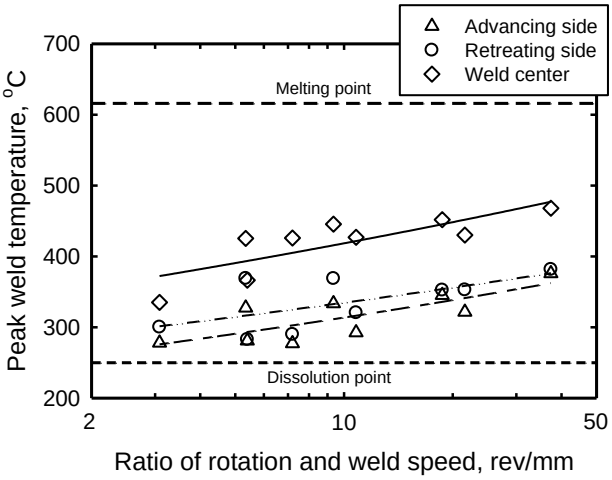

Figure 4. Relation of peak weld temperatures with the ratio of tool rotation speed and weld speed (ω/v)

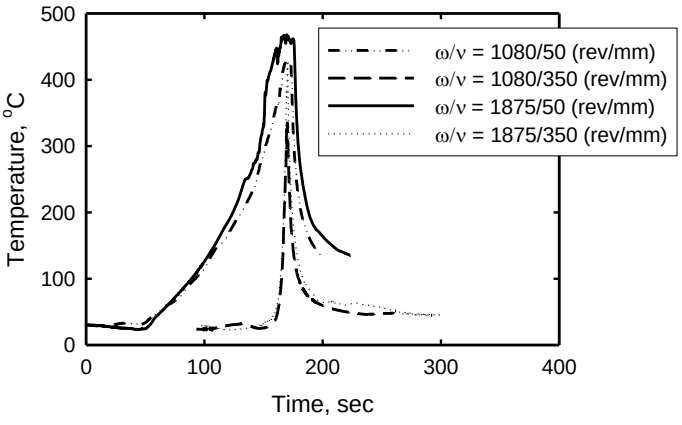

Figure 5. Effect of weld parameters on the thermal cycle at the end weld center of the FSWs

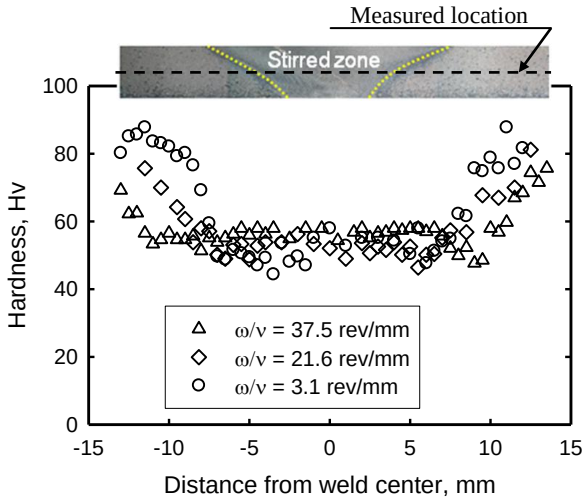

Figure 6. Hardness in the cross section of the FSW under different weld conditions

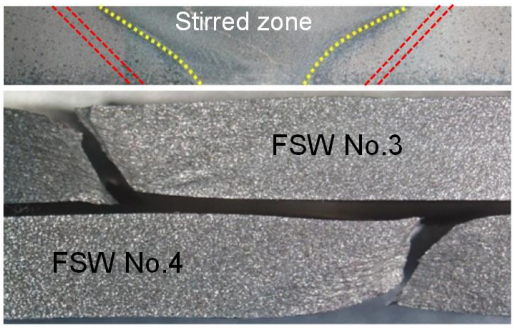

Figure 7. Cross sections and the tensile fracture locations in FSW No.3 (ω/v = 7.2 rev./mm) and FSW No.4 (ω/v = 5.4 rev./mm) (Advacing side and retreating side are in the left side and right side, respectively)

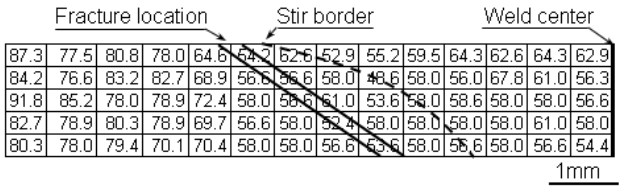

Figure 8. Hardness distribution in cross section of FSW No.3

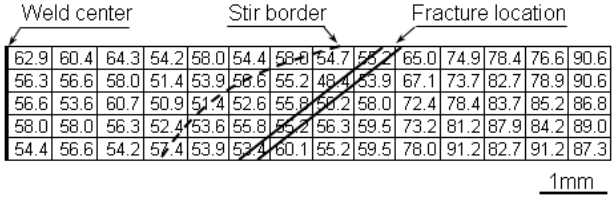

Figure 9. Hardness distribution in cross section of FSW No.4

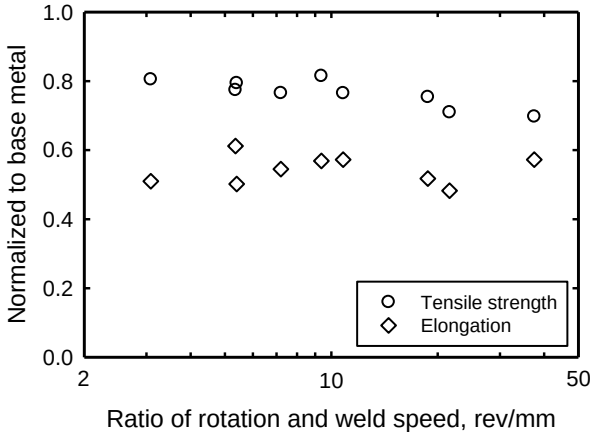

Figure 10. Elongation and tensile strength of FSWs normalized to these of BM under various weld conditions

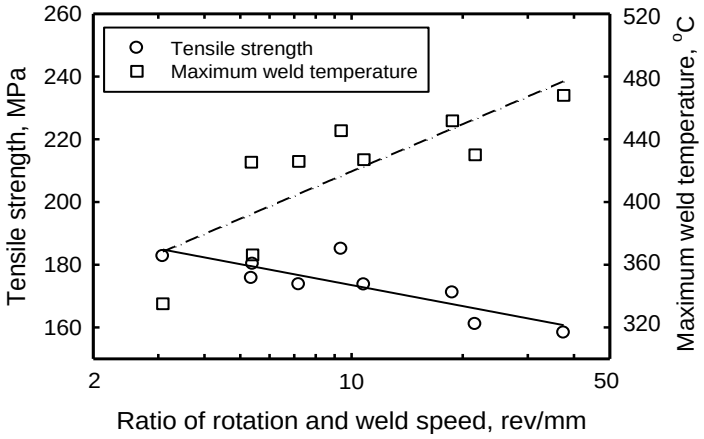

Figure 11. Relation of tensile strength and weld temperature with the ratio of rotation speed and weld speed

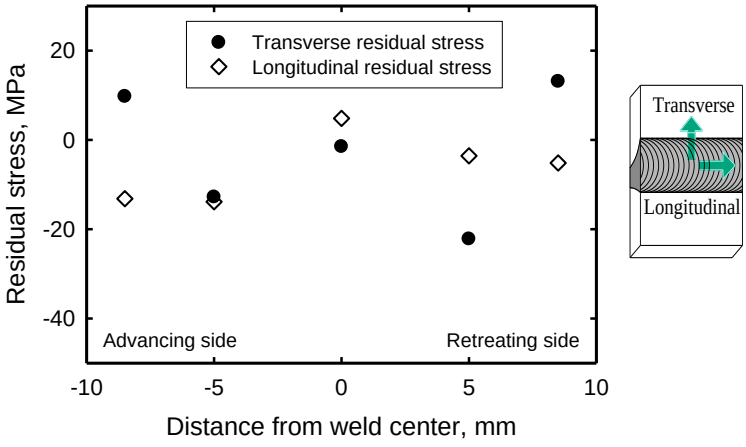

Figure 12. Residual stress in and around the welded zone

The tensile strength of the FSW 6063-T5 was carried out by the MTS hydraulic machine at a constant strain rate of 10^{-3}/s by means of the specimen shown in Figure 1. The tensile failures of all FSW specimens took place at the HAZ in the advancing side or in the retreating side as seen in Figure 7. It should be noted that all tensile failures were occurred outside the stirred zone. The tensile fracture locations were well agreement with the lowest hardness locations as seen in Figure 8 and Figure 9 (the locations of solid-lines).

The results of tensile strength and elongation under various weld conditions, normalized to these of BM, are presented in Figure 10. In all weld conditions, the tensile property of the FSW was lower than that of BM. Generally, the tensile strength and elongation of the FSWs are about 75% and 55% that of BM, respectively. The influence of weld parameters on tensile strength of the FSW can be seen in Figure 11. Here, the tensile strength is reduced when the weld parameter ω/v is increased. This reduction of tensile strength could be concerned with the higher heat input during the welding process as seen in Figure 11 that must be resulting from the dissolution and/or coarsening of precipitates in and around the welded zone of this alloy (see the dissolution point in Figure 4). It is necessary to note that the FSW fabrication at low value of ω/v could lead to the incomplete joint, *i.e.*, ω/v = 2.5 rev/mm.

Finally, the residual stress in and around of the welded zone of a FSW (fabricated at ω/v = 3.1 rev/mm) was examined by X-ray diffraction technique. The measured results of the transverse and longitudinal residual stress are shown in Figure 12 in which each value is averaged from three measurements. The result in Figure 12 approved that the FSW could be obtained with quite low residual stress. Here, both longitudinal and transverse residual stresses were in range of about ten percent of yield stress of BM.

Conclusions

The FSW of aluminum alloy 6063-T5 was fabricated and the effect of weld parameters on its thermal cycles, hardness, and tensile properties was investigated. The heat input was found to be proportional to the ratio of tool rotation speed and weld speed, ν/ω . The lower the ratio of rotation speed and weld speed, the higher tensile strength were. The tensile fracture located outside the stirred zone, in the retreating side or advancing side, where the hardness was lowest. The kissing bond defects seem to be inevitable in all most all of cases excepting for a high value of ν/ω (*i.e.*, 37.5 rev/min) there the weld surface was deformed turbulently. The FSW joint could be obtained with quite low residual stress.

Acknowledgments

The author is grateful to Professor Masakazu Okazaki for his guidance and experimental equipment support. The author also thanks to Professor Kenji Suzuki for his support in the residual stress measurement.

References

[1] M. Gene, *The Welding of Aluminium and its Alloys*, Woodhead Publishing Ltd., Cambridge, England, 2002.

[2] H.T. Tran, M. Seino, M. Sakaguchi, and M. Okazaki, "Fatigue crack propagation behavior relevant to inhomogeneous microstructure of friction stir welding AA6063-T5," *Journal of Solid Mechanics and Materials Engineering*, Vol. 4, No. 6, pp. 840-848, 2010.

[3] M. Sakaguchi, A. Sano, H.T. Tran, M. Okazaki, and M. Sekihara, "Low cycle and thermal-mechanical fatigue of friction welded dissimilar super alloys joint," *Journal of Solid Mechanics and Materials Engineering*, Vol. 2, No. 12, pp. 1508-1516, 2008.

[4] Z.Y. Ma, "Friction stir processing technology: A Review," *Metallurgical and Materials Transactions*, Vol. 39, No. 3, pp. 642-658, 2008.
[5] T. Morishige, M. Tsujikawa, M. Hino, T. Hirata, S. Oki, and K. Higashi, "Microstructural modification of cast Mg alloys by friction stir processing," *International Journal of Cast Metals Research*, Vol. 21, No. 1-4, pp. 109-113, 2008.
[6] J.Q. Su, T.W. Nelson, and C.J. Sterling, "Grain refinement of aluminum alloys by friction stir processing," *Philosophical Magazine*, Vol. 86, No. 1, pp. 1-24, 2006.
[7] Y. Morisada, H. Fujii, T. Mizuno, G. Abe, T. Nagaoka, and M. Fukusumi, "Modification of nitride layer on cold-work tool steel by laser melting and friction stir processing," *Surface and Coatings Technology*, Vol. 204, No. 3, pp. 386-390, 2009.
[8] R.S. Mishra, and M.W. Mahoney, ed., *Friction Stir Welding and Processing*, American Society for Metals (ASM) International, 2007.
[9] D.P. Field, T.W. Nelson, Y. Hovanski, and K.V. Jata, "Heterogeneity of crystallographic texture in friction stir welds of aluminum," *Metallurgical and Materials Transactions A: Physical Metallurgy and Materials Science*, Vol. 32, No. 11, pp. 2869-2877, 2001.
[10] R.W. Ponda, and J.F. Bingert, "Precipitation and grain refinement in a 2195 Al friction stir weld," *Metallurgical and Materials Transactions A: Physical Metallurgy and Materials Science*, Vol. 37, pp. 3593-3604, 2006.
[11] A. Oosterkamp, L.D. Oosterkamp, and A. Nordeide, "'Kissing bond' phenomena in solid-state welds of aluminum alloys," *Welding Journal (Miami, Florida, United States)*, Vol. 83, No. 8, pp. 225-231, 2004.
[12] The Society of Materials Science of Japan, *Standard Method for X-Ray Stress Measurement (JSMS-SD-10-05)*, Kyoto, Japan, 2005.
[13] W. Tang, X. Guo, J.C. McClure, L.E. Murr, and A. Nunes, "Heat input and temperature distribution in friction stir welding," *Journal of Materials Processing and Manufacturing Science*, Vol. 7, pp. 163-172, 1998.
[14] Y.S. Sato, H. Kokawa, M. Enomoto, S. Jogan, and T. "Hashimoto, Precipitation sequence in friction stir weld of 6063 aluminum during aging," *Metallurgical and Materials Transactions A*, Vol. 30, No. 12, pp. 3125-3130, 1999.
[15] W.D. Callister, *Materials Science and Engineering - An Introduction*, John Wiley & Sons, Inc., New York, United States, 2007.